Received: 10 March 2021 | Revised: 26 August 2021 | Accepted: 15 September 2021

DOI: 10.1002/ppul.25684

ORIGINAL ARTICLE: INFECTION AND IMMUNITY

PEDIATRIC PULMONOLOGY WILEY

Early-onset, fatal interstitial lung disease in STAT3 gain-of-function patients

Florian Gothe MD[1] | Jonathan Gehrig BSc[2] | Christina K. Rapp MSc[1] | Katrin Knoflach MD[1] | Simone Reu-Hofer MD[3] | Florian Länger MD[4,5] | Dirk Schramm MD[6] | Julia Ley-Zaporozhan MD[7] | Stephan Ehl MD[2,8] | Nicolaus Schwerk MD[5,9] | Laura Faletti PhD[2,8] | Matthias Griese MD[1,10]

[1]Department of Pediatrics, Dr. von Hauner Children's Hospital, University Hospital, Ludwig-Maximilians-Universität Munich, Munich, Germany

[2]Center for Chronic Immunodeficiency, Medical Center, Institute for Immunodeficiency, University of Freiburg, Freiburg, Germany

[3]Department of Pathology, Julius-Maximilians-Universität Wuerzburg, Wuerzburg, Germany

[4]Department of Pathology, Hannover Medical School, Hanover, Germany

[5]German Center for Lung Research (DZL), BREATH Hannover, Hanover, Germany

[6]Department of Pediatric Pneumology, University Children's Hospital Düsseldorf, Düsseldorf, Germany

[7]Department of Radiology, Pediatric Radiology, University Hospital, Ludwig-Maximilians-Universität Munich, Munich, Germany

[8]Centre for Integrative Biological Signalling Studies (CIBSS), University of Freiburg, Freiburg, Germany

[9]Department of Pediatric Pulmonology, Allergology and Neonatology, Hannover Medical School, Hanover, Germany

[10]German Center for Lung Research (DZL), CPC Munich, Munich, Germany

Correspondence
Florian Gothe, MD, and Matthias Griese, MD, Department of Pediatrics, Dr. von Hauner Children's Hospital, University Hospital, Ludwig-Maximilians-Universität Munich, Lindwurmstr. 4, 80337 Munich, Germany.
Email: florian.gothe@med.uni-muenchen.de and matthias.griese@med.uni-muenchen.de

Funding information
Care-for-Rare Foundation; ERA-Net for Research on Rare Diseases; Munich Clinician Scientist Program; Deutsche Forschungsgemeinschaft, Grant/Award Numbers: 390939984 and, Gr970/9-1; German Center for Lung Research; Bundesministerium für Bildung und Forschung, Grant/Award Numbers: 01GM1910A and, HCQ4Surfdefect

Abstract

Gain-of-function variants in *STAT3* are known to cause severe, multifaceted autoimmunity. Here we report three individuals with de-novo *STAT3 GOF* alleles and early-onset, severe interstitial lung disease manifesting during the first 3 years of life. Imaging and histology revealed different forms of interstitial pneumonia alongside fibrotic and cystic tissue destruction. Definitive diagnosis was established by postmortem whole exome sequencing and functional validation of two new *STAT3* variants. Such lung-predominant forms of *STAT3 GOF* disease expand the phenotypic spectrum of diseases associated with activating *STAT3* variants and add to our understanding of this life-threatening inborn error of immunity.

Keywords:
autoimmunity, inborn error of immunity, interstitial lung disease, STAT3

Florian Gothe, Jonathan Gehrig, Laura Faletti, and Matthias Griese contributed equally to this work.

1 | INTRODUCTION

Germline activating variants in *Signal transducer and activator of transcription 3* (*STAT3*) have been reported to cause severe immune dysregulation with variable expressivity and incomplete penetrance.[1,2] Notably, in most of the cases published, mutations occurred de-novo.[3] With disease onset at a mean age of 3 years, multisystem autoimmunity frequently manifests with cytopenias, enteropathy and endocrinopathies like type I diabetes.[3,4] In about a third of individuals, interstitial lung disease (ILD) is observed, usually starting in adolescence.[3] However, lung involvement is rarely reported as the clinically dominant symptom and data on precise lung histology and imaging phenotypes is sparse.

Here we report three pediatric cases of severe and ultimately fatal ILD, followed in the child-EU registry and diagnosed postmortem to carry heterozygous gain-of-function (GOF) variants in *STAT3*. Functional validation of two new variants and in-depth histological and imaging studies highlight the clinical features that might alert pulmonologists taking care of patients with early-onset ILD to the possibility of this diagnosis.

2 | METHODS

2.1 | Human subjects

Informed consent was provided by all human subjects or their legal guardians in accordance with the 1975 Helsinki principles for enrollment in research protocols that were approved by the Institutional Review Board of the LMU Munich (EK 15032011). Patients I and II were additionally followed in the child-EU registry and local Institutional Review Boards had approved its consent forms (EK 20-0329).

2.2 | Cell culture

The STAT3 deficient human colon carcinoma cell line A4[5] was cultured in McCoy's 5a medium (Gibco by Thermo Fisher Scientific Inc.) supplemented with 5% (v/v) FCS (Sigma-Aldrich) and 1% (v/v) penicillin-streptomycin (Sigma-Aldrich) at 37°C and 5% CO_2. A4 cells were stably transduced with *STAT3* wild-type (WT) or mutant alleles by retroviral transduction as described before.[5]

2.3 | Cloning

Different *STAT3* alleles were generated by site-directed mutagenesis from the WT *STAT3* using mutation specific primers (Table E1). The *STAT3* variants were introduced into the pMX-IRES-eGFP vector.

2.4 | Luciferase reporter assay

A4 cells were seeded in 24-well plates and transiently transfected after 24 h using the Promofectin (PromoKine) transfection protocol. For this, cells were transfected with 250 ng pmX-IRES-GFP expression plasmid containing *STAT3* WT or mutant variant, 150 ng pUC18 carrier DNA and 100 ng of a STAT3-responsive Firefly reporter (5'-GTCGACATTTCCC GTAAATCGTCGAGTCGA-3') premixed with a Renilla expression plasmid (Cignal STAT3; Qiagen). Forty-two hours after transfection, cells were stimulated with 10 ng/ml interleukin-6 (IL6; Peprotech) for 6 h. Cells were harvested and Firefly and Renilla luciferase activity were measured using the Dual-luciferase reporter assay kit (Promega). Firefly luciferase activity was normalized to Renilla luciferase activity and the fold change compared with unstimulated WT cells was calculated.

2.5 | DNA binding assay

Transduced A4 cells were stimulated with 10 ng/ml IL6 for 30 min. Nuclear extraction was performed using the Nuclear Extract Kit (ActiveMotif) according to the manufacturer's guideline. DNA binding to the motif 5'-TTCCCGGAA-3' was assessed with the TransAM® STAT3 Kit (ActiveMotif).

2.6 | RNA isolation, complementary DNA (cDNA) synthesis, and real-time quantitative reverse-transcription polymerase chain reaction (RT-PCR)

RNA isolation was performed with the RNeasy Micro Kit (Qiagen) according to the manufacturer's guideline. For cDNA synthesis the qScript cDNA Supermix (Quantabio) was used. Real-time quantitative RT-PCR was done with the Mastercycler Realplex instrument (Eppendorf). For the PCR reaction, FastStart Universal SYBR Green Master (Rox) (Roche) was mixed with 0.5 µM primer (listed in Table E1) and 5 µl cDNA. For gene expression analyses, data were normalized to *SDHA* gene expression and calculated with the $\Delta\Delta C_t$ method.

2.7 | Sodium dodecyl sulfate–polyacrylamide gel electrophoresis (SDS-PAGE) and Western blot analysis for dephosphorylation kinetics

Transiently transfected A4 cells were stimulated with IL6 for 15 min before the cytokine was washed away. Cells were harvested either directly or after another 45 or 105 min in media, resuspended in lysis buffer (50 mM Tris/HCl 8; 150 mM NaCl; 5 mM $MgCl_2$; 0.1% NP40, 1× protease inhibitor [Roche]; 1 mM DTT; 1:100 Phosphatase Inhibitor Cocktail 2 [Sigma-Aldrich]) and incubated on ice for 30 min. Lysates were cleared from cellular debris by centrifugation (16,000*g*, 5 min, 4°C). Proteins were separated by SDS-PAGE, transferred onto Nitrocellulose membranes and detected with anti-phospho-Stat3 (Tyr705) (1:2000, #9145; Cell Signaling Technology) and anti-Stat3 (1:1000, #9139; Cell Signaling Technology) antibodies. The bands signal intensities were quantified with the Fusion software. Phospho-Stat3 signal was normalized to Stat3 signal and the fold change pSTAT3/STAT3 ratio relative to unstimulated was calculated for comparison.

TABLE 1 Clinical characteristics of the patients

Patient	1	2	3
Variant in *STAT3*	c.1847A>T, p.E616V	c.1276T>C, p.C426R	c.1275T>A, p.N425K
Gender	Female	Male	Female
Ethnic origin	Caucasian	Half Caucasian—Half African	Caucasian
Age at death (years)	2	14	12
Respiratory findings			
Onset of lung symptoms (years)	2	2	3
Respiratory symptoms	Dry cough, wheezing, hypoxia	Clubbing, tachypnea, retractions, hypoxia	Cough, clubbing, tachy-pnea, retractions, hypoxia
Recurrent respiratory infections	–	+	–
Lung function at first evaluation (see also Figure 1C)	–	FEV1 58%, FVC 54%, TLCOc 21%	FEV1 45%, FVC 53%
Bronchoalveolar lavage	Inflammation with mostly $CD8^+$ lymphocytes (35%), macrophages (31%), neutrophils (28%), Rhinovirus/CMV-PCR pos.	Inflammation with macrophages (41%) $CD8^+$ lymphocytes (33%), neutrophils (11%), eosinophils (13%)	Inflammation with macrophages (59%), mostly $CD8^+$ lymphocytes (21%), eosinophils (12%), neutrophils (8%), EBV-PCR pos.
Lung histology	NSIP: mild interstitial inflammatory infiltrate, small lymphoid aggregates, increased alveolar macrophages, chronic bronchiolitis, no fibrosis	LIP: irregularly enlarged airspaces, diffuse moderate lymphocytic interstitial infiltrate with few lymphoid follicles, mild interstitial fibrosis	NSIP: mild to moderate lymphocytic interstitial infiltrate with few plasma cells, mild loose fibrosis
Chest CT imaging	Patchy GGO, intralobular septal thickening	Multiple singular and clustered cystic lucencies in random distribution	Cystic lung destruction, dilatated central bronchi, bronchial wall thickening, traction bronchiectasis
Other features			
Lymphadenopathy	+	+	+
Splenomegaly	–	+	+
Hepatomegaly	–	–	–
Malignancy	–	–	–
Anemia	–	–	–
Thrombocytopenia	–	–	–
Neutropenia	–	–	–
Inflammatory gut disease/enteropathy	–	+	+
Inflammatory skin disease	Atopic eczema	Atopic eczema	Atopic eczema
Other autoimmunity/immune dysregulation	–	Polyarthritis, diabetes, alopecia	Recurrent episodes of kidney stones
Recurrrent infections	–	EBV-PCR pos. in blood	EBV-PCR pos. in blood
Hypogammaglobulinaemia	–	–	–
Short statue/Failure to thrive	–	+	+
Treatment			
Corticosteroids	+	+	+
Rituximab	–	–	+

TABLE 1 (Continued)

Patient	1	2	3
Other medication	–	Azithromycin, Hydroxy-chloroquin, Anti-TNFa, MMF	Azathioprine, Cyclophosphamide
IVIG	–	+	+

Abbreviations: CD8, cluster of differentiation; CMV, cytomegalovirus; EBV, Epstein–Barr virus; FEV1, forced expiratory volume; FVC, forced vital capacity; GGO, ground glass opacities; IVIG, intravenous immunoglobulins; LIP, lymphoid interstitial pneumonia; MMF, mycophenolate mofetil; NSIP, nonspecific interstitial pneumonia; TNFa, tumor necrosis factor α; TLCOc, transfer factor of the lung for carbon monoxide.

2.8 | Statistics

For statistical analyses the one-way analysis of variance with Dunnett's posthoc test was used. Significant changes are indicated by $^{*}p < 0.05$; $^{**}p < 0.01$ $^{***}p < 0.001$ and $^{****}p < 0.0001$.

3 | RESULTS

3.1 | Case descriptions

Patient 1 came to medical attention shortly after her second birthday, presenting with dry cough, wheezing and exercise intolerance. Her medical history was unremarkable except for atopic eczema in infancy. The initial diagnostic work-up revealed no signs of allergic sensitization but bronchoalveolar lavage (BAL) fluid analysis showed an increased frequency of $CD8^+$ lymphocytes. Additionally, high levels of *Rhinovirus* RNA (500.000 copies/ml) and low levels of *Cytomegalovirus* (CMV) DNA (2.000 copies/ml) were detected by PCR (Table 1). Computed tomography (CT) imaging of the chest showed diffuse patchy ground glass opacities (GGO) with mild intralobular septal thickening (Figure 1A). Lung biopsy revealed a diffuse mild to moderate interstitial inflammatory infiltrate and few very small lymphoid aggregates without lymphoid follicles most consistent with a cellular nonspecific interstitial pneumonitis (NSIP) pattern (Figure 1E). Significant interstitial fibrosis was not seen. CMV-immunohistochemistry was negative and viral inclusion bodies were also not observed. Immune phenotyping revealed normal lymphocyte subpopulations. Anti-nuclear antibodies (ANAs), anti-neutrophil cytoplasmic antibodies or granulocyte-macrophage colony-stimulating factor (GM-CSF) autoantibodies were not detected (Table E2). She was managed with steroids, but her clinical condition deteriorated within weeks. After the start of ganciclovir CMV was no longer detectable in tracheal aspirates, however, the patient developed a systemic inflammatory response syndrome (SIRS) with high C-reactive protein levels (CRP, up to 300 mg/L) and subsequent acute respiratory distress syndrome (ARDS). Therefore, a veno-venous extracorporal membrane oxygenation (vvECMO) was put in place, but as a complication of anticoagulation, the patient experienced massive intracranial bleeding four days later leading to her death. Unfortunately, the parents declined a postmortem examination and so we can only speculate whether the rapidly progressive lung disease might have been triggered by viral infection.

Patient 2 also suffered from atopic eczema during his first year of life. From the age of 2 years onwards, recurrent pneumonias and episodes of airway obstruction were diagnosed. Analyzing the patient's medical record retrospectively, it appeared that fever and elevated CRP values were rarely present on these occasions, but pleural effusions and signs of atypical pneumonia were noted on chest X-rays. By 5 years of age, clubbing was noted. During the following years, the patient was treated for presumed asthma and multisystemic autoimmune features like inflammatory bowel disease, type I diabetes, severe polyarthritis, and alopecia occurred (Table 1). Extensive immunological investigations showed mildly reduced T cell numbers with a normal $CD4^+/CD8^+$ ratio as well as reduced class-switched memory B cells despite normal specific antibody levels. ANAs or other autoantibodies were not detected. At this point, constantly elevated CRP levels and increased soluble Interleukin-2 receptor levels (maximum 5.375 kU/L) were noted indicating chronic inflammation. Multiple inborn errors of immunity including X-linked lymphopoliferative syndromes, familial hemophagocytic lymphohistiocytosis and Wiskott–Aldrich syndrome had been ruled out by specific flow cytometric assays. At the age of 10, he presented hypoxemic and lung function testing revealed a severe combined obstructive-restrictive pattern alongside a carbon monoxide-diffusion capacity of 21% (Table 1, Figure 2). He was treated with steroid pulses plus additional hydroxychloroquine and azithromycin. Lung biopsy indicated lymphoid interstitial pneumonia (LIP) with irregularly enlarged airways and mild interstitial fibrosis (Figure 1F). BAL demonstrated moderate lymphocytic inflammation with 95% of lymphocytes being CD8 positive. He became oxygen-dependent at the age of 12 and received a double lung-transplant at the age of 13. Eleven months posttransplant his clinical status deteriorated rapidly with CT scanning revealing diffuse, bilateral GGOs. While no infectious agent could be identified, new donor-specific antibodies were detected. Lung transplant biopsy was consistent with humoral rejection revealing no signs of bronchiolitis obliterans or cellular rejection. When comparing the transplant biopsy with the explanted lung tissue, pathologists argued against a potential relapse of the underlying disease in the allograft. Despite extensive treatment (methylprednisolone, rituximab, intravenous immunoglobulins, extracorporal immunoadsorption, alemtuzumab), the patient died two months later of progressive respiratory failure.

In Patient 3, atopic eczema was also the first sign of immune dysregulation. She was treated for suspected pneumonia at the age of 3 when chronic dry cough and clubbing were noted. At 7 years of age, a severe restrictive lung function and secondary pulmonary hypertension were diagnosed (Figure 2). Systemic steroid and

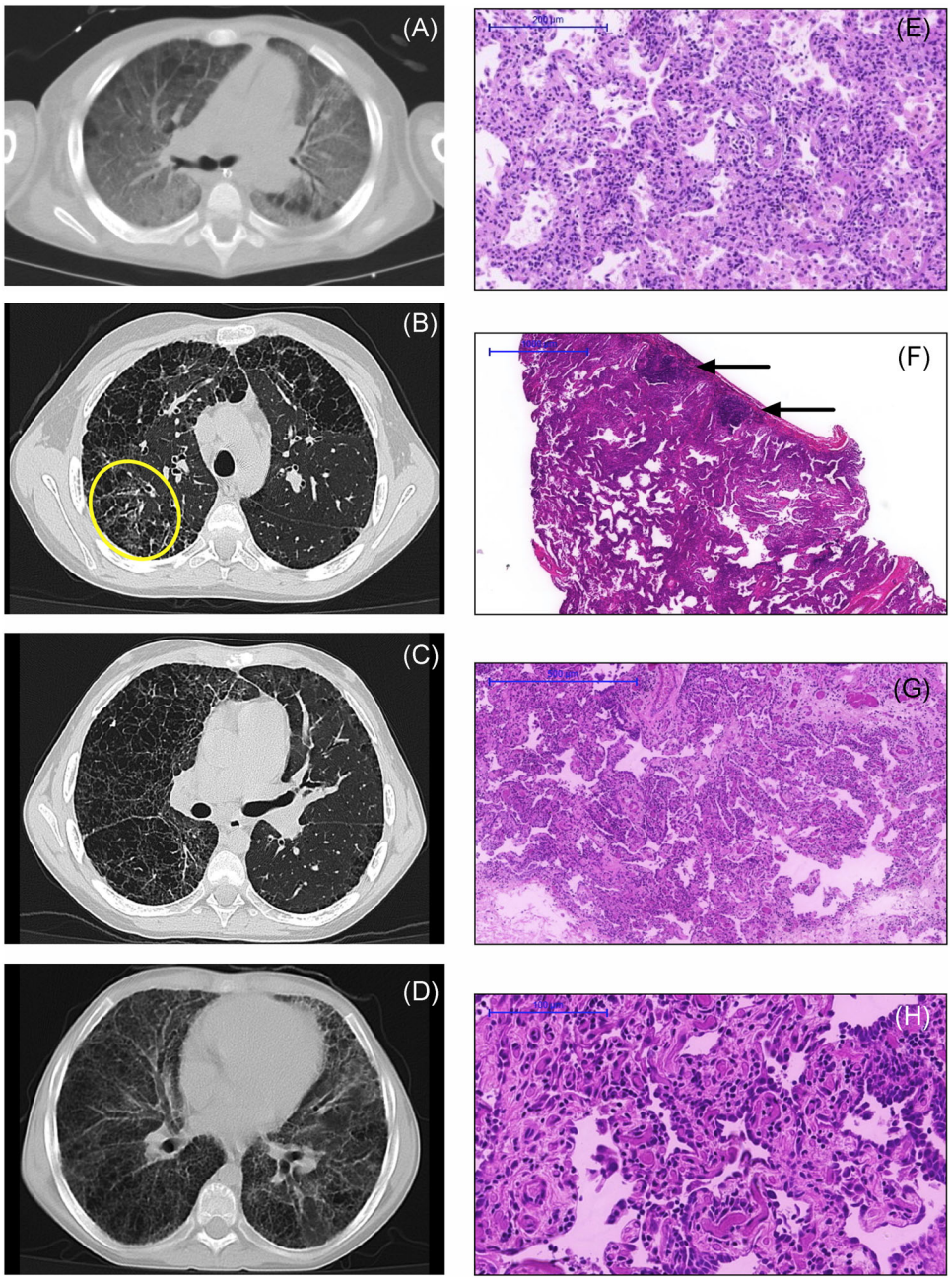

FIGURE 1 Multimodal assessment of the lung. Chest CT scans in patient 1 (A) and two consecutive CT studies in patient 3 at the age of 10 (B and C) and 11 (D) years, respectively. The yellow circle indicates traction bronchiectasis. Lung histology in patient 1 (E, H&E ×100), patient 2 (F, H&E ×20) with the arrows highlighting lymphoid follicles. Lymphocytic infiltrates in patient 3 (G, H&E ×50 and H, H&E ×200). CT, computed tomography; LTx, lung transplantation [Color figure can be viewed at wileyonlinelibrary.com]

azathioprine treatment were commenced, the latter switched to cyclophosphamide later. Lung biopsy revealed cellular NSIP pattern and interstitial fibrosis (Figure 1G,H). In the BAL, moderate inflammation with mostly $CD8^+$ lymphocytes was noted. At 10 years of age, oxygen supplementation was initiated. CT imaging (Figure 1B,C) displayed cystic lung destruction, dilatated central bronchi with mild bronchial wall thickening and traction bronchiectasis. Worsening of bronchiectasis was evident within 12 months (Figure 1D). Immunologic evaluation revealed normal T cell numbers with an inverted $CD4^+/CD8^+$ ratio (0.4) and constantly reduced NK cell frequencies (2% of lymphocytes). IgG subclasses as well as specific antibody production appeared normal and autoantibodies were not detected (Table E2). However, fluctuating and often elevated CRP levels suggested systemic inflammation. Progressive respiratory failure with frequent exacerbations preceded a trial with Rituximab alongside intravenous immunoglobulins. However, acute right heart failure occurred and despite iloprost, sildenafil and nitric oxide treatment the patient died of cardiac and liver failure at the age of 11.

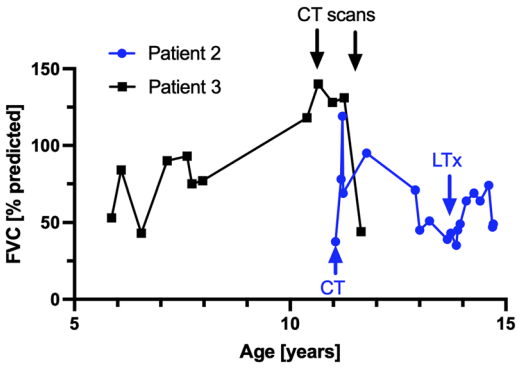

FIGURE 2 Lung function over time. FVC courses in patients 2 (blue) and 3 (black). FVC, forced vital capacity [Color figure can be viewed at wileyonlinelibrary.com]

3.2 | Genetic evaluation and functional validation

Whole exome sequencing (WES) performed retrospectively revealed heterozygous *STAT3* missense variants in all three patients; two of them novel (E616V in P1 and N425K in P3), one previously described (C426R in P2) (Figure 3A). We investigated the functional consequences of these variants by introducing them into the STAT3-deficient cell line A4. First, STAT3-deficient A4 cells were transfected with the patient-derived *STAT3* alleles and a STAT3-responsive luciferase reporter. After treating the cells with or without IL-6, the expression of the luciferase reporter gene was measured to quantify the activity of the STAT3 promoter. The E616V variant displayed increased baseline transcriptional activity (Figure 3B). No increase in baseline or IL6-induced reporter activity was observed for N425K or C426R. This has been previously described for

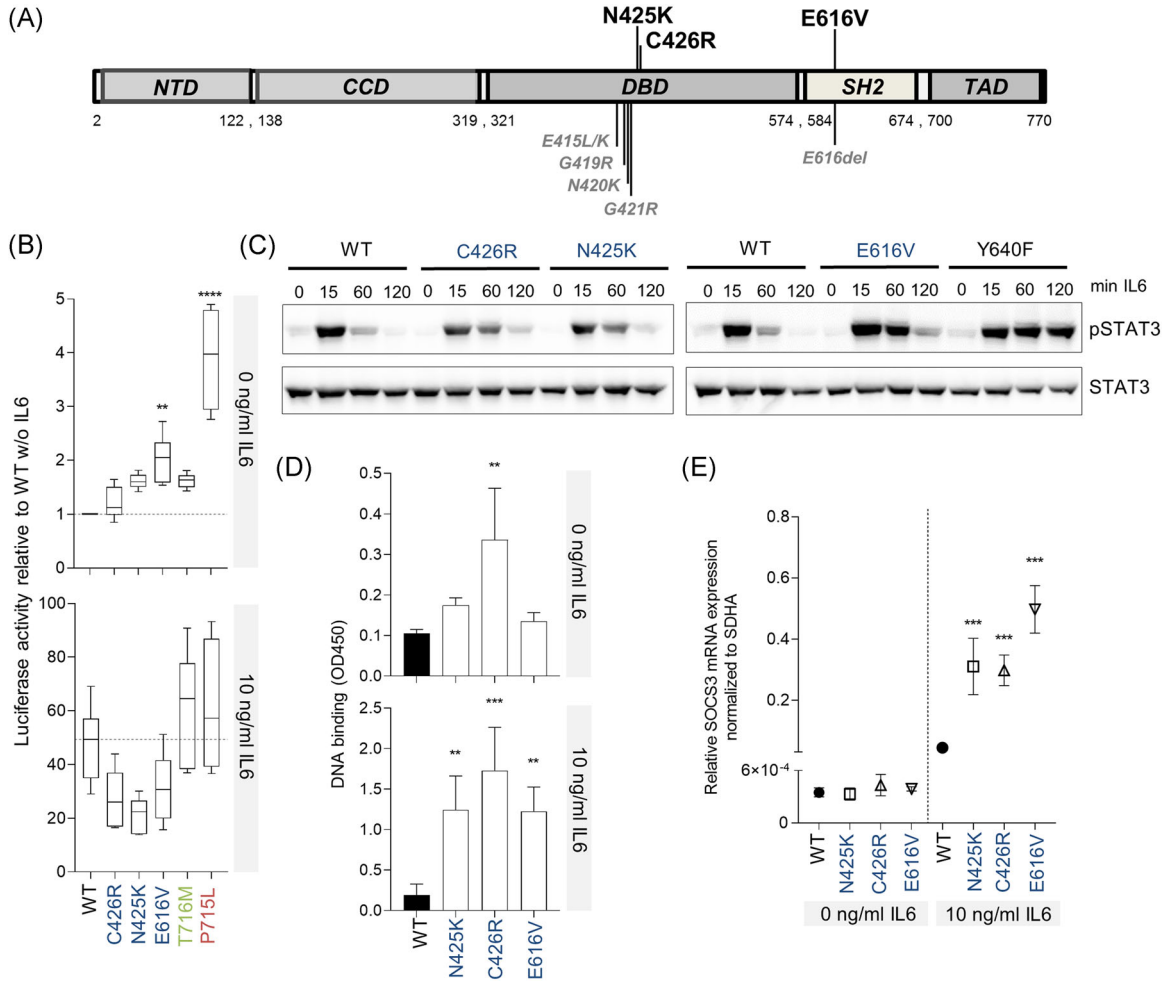

FIGURE 3 Molecular characteristics of N425K and E616V STAT3 variants. (A) Schematic of the STAT3 protein including the variants found in this study (top) and known variants located in close proximity (bottom). Luciferase reporter assay (B) and dephosphorylation kinetics (C) in *STAT3* deficient A4 cells transfected with STAT3 WT or STAT3 mutant plasmids. Box plots show the relative luciferase activity compared with WT without IL-6 stimulation. Representative western blot of pSTAT3-Y705/total STAT3 levels after IL-6 stimulation (10 ng/ml) for the indicated times, $n = 3–4$. Binding of STAT3 to the DNA (D) and expression of SOCS3 (E) in *STAT3* deficient A4 cells stably transduced with *STAT3* WT or *STAT3* mutant plasmids. For statistical analyses a one-way ANOVA with Dunnett's posthoc test was performed. Significant changes are indicated by $^{*}p < 0.05$; $^{**}p < 0.01$, and $^{***}p < 0.001$. P715L, T716M, C426R and Y640F variants were used as positive controls. Red: group 1 mutants, green: group 2 mutants and blue: group 3 mutants. *NTD: N-terminal domain; CCD: Coiled-coil domain; DBD: DNA-binding domain; SH2: Src homology 2 domain; TAD: Transactivation domain. [Color figure can be viewed at* wileyonlinelibrary.com]

some clinically relevant *STAT3* alleles, which were GOF in other assays.[5] The previously reported P715L and T716M *STAT3* GOF variants were used as additional positive controls. To further explore the molecular behavior of the variants, we investigated the kinetics of STAT3 dephosphorylation following IL-6 stimulation. The dephosphorylation was slightly delayed for all three mutants in comparison to the WT (Figure 3C). The large granular leukemia (LGL)-associated Y640F *STAT3* GOF variant was used as positive control in this assay. We next tested the DNA binding capacity of the *STAT3* mutants to the DNA sequence motif 5′-TTCCCGGAA-3′ (Figure 3D) using ELISA. To do so, A4 cells were stably transduced with the WT and the *STAT3* mutants. As previously reported by Jägle et al.,[5] the C426R variant showed increased baseline DNA binding (Figure 3D, upper panel). Upon IL-6 stimulation, all variants displayed a significant increase in DNA binding compared with the WT STAT3 (Figure 3D, lower panel). Finally, the transcriptional induction of suppressor of cytokine signaling 3 (SOCS3) (Figure 3E) was assessed in the stably transduced A4 cell lines. The two new mutations (N425K and E616V) and the already known C426R showed a significant increase in SOCS3 mRNA upon IL-6 stimulation, clearly demonstrating a GOF behavior.

4 | DISCUSSION

In the three cases presented here, symptoms of severe ILD started during the first 3 years of life and determined the ultimately fatal disease outcome. At the time of death, the disease entity STAT3 GOF had either not been described (in two patients) or the gene had not been added to WES panels. Notably, none of the patients displayed autoimmune cytopenias, the most frequent organ manifestation of STAT3 GOF disease.[3]

Interestingly, neither radiologic evaluation nor lung histology revealed a uniform pattern which could aid diagnosis. Chest CT scans displayed GGOs, cystic lesions and bronchiectasis at varying degrees. Histopathologic examination revealed either a cellular NSIP or LIP pattern, both of which have been reported in one or three STAT3 GOF individuals respectively.[6,7] Interstitial fibrosis, as seen in patient 3, has not been observed in a recently published, detailed histopathologic report of two cases.[7] BAL cytology suggested moderate lymphocytic inflammation with large predominance of CD8 expressing lymphocytes in all three patients. Such lymphocytosis with inverted CD4/CD8 ratio in BAL is, however, not disease-specific and has for example been reported in paediatric patients suffering from hypersensitivity pneumonitis.[8] Whether lung pathology is related to increased STAT3 activity in lung fibroblasts[9–11] or consequence of unrestrained immune cell activation, for example, in the absence of sufficient regulatory T cell (Treg) capacity, is not yet clear. However, ILD phenotypes have been reported in different inborn errors of immunity (IEI) associated with Treg dysfunction besides STAT3 GOF disease,[2] that is, IL2RB deficiency,[12] CD25 deficiency,[13] IPEX syndrome,[14] CTLA4 haploinsufficiency[15] or LRBA deficiency.[16] In addition, pulmonary involvement is also a prominent feature of monogenic autoinflammatory disorders affecting the regulation of type I interferon signaling, for example, SAVI syndrome,[17] COPA syndrome[18,19] or OAS1 GOF disease.[20] It is therefore mandatory to consider these IEIs in children with ILD onset before the age of 3 years, especially when additional signs of immune dysregulation like eczema or organ-specific autoimmunity, most evident in the clinical course of case 2, are present. In addition to standard immune function assays, Treg enumeration and interferon scores appear to be valuable screening tests.[21] In the BAL of our three cases, a consistent increase in cytotoxic T cell frequencies was noted and albeit being nonspecific, this might be useful as a diagnostic hint.

Nevertheless, a definite molecular diagnosis should be scrutinized by genetic testing (ideally using a whole exome sequencing approach) early in the disease course followed by thorough functional validation of observed variants. To validate the GOF behavior of the mutations we used four different experimental approaches. Interestingly, the two new variants (N425K and E616V) displayed a reduced luciferase reporter activity following IL-6 stimulation when compared with the WT allele. However, delayed STAT3 dephosphorylation as well as significant increases in DNA binding and SOCS3 expression clearly demonstrate GOF effects in both variants. This is in line with our previous studies where the GOF effect of some *STAT3* variants could not be detected in the luciferase reporter assay.[5] This might be due to the fact that the luciferase reporter assay uses only one of several STAT3 binding DNA sequence elements. Of note, there are additional patients carrying group 3 alleles (C426R and E415L), as defined by Jägle et al., who have been reported to suffer from ILD.[5,22,23] More patients are needed to assess whether group 3 variants, which show the strongest DNA-binding capacity, are associated with a higher risk of pulmonary involvement.

Diagnosing STAT3 GOF situations in a timely manner is of utmost importance since targeted therapies are available. Janus tyrosine kinase inhibitors blocking signaling downstream of the IL-6 receptor amongst others have recently been found effective in stabilizing pulmonary function of four STAT3 GOF patients.[6] In addition, this report illustrates the need to closely monitor pulmonary function in all patients diagnosed to carry STAT3 GOF alleles.

ACKNOWLEDGMENTS

F. G. was supported by the Munich Clinician Scientist Program (FoeFoLeplus) and the Care-4-Rare-Foundation. S. E., L. F. and J. G. were supported by the German Research Foundation (DFG) under Germany's Excellence Strategy (CIBSS—EXC-2189 grant number 390939984) and the German Federal Ministry of Education and Research (BMBF) GAIN-consortium (TP6; grant number 01GM1910A). The work of M. G. was supported by the DFG (grant number Gr 970/9-1), the BMBF ("HCQ4Surfdefect") under the frame of E-Rare-3, the ERA-Net for Research on Rare Diseases and the German Center for Lung Research (DZL). Open Access funding enabled and organized by Projekt DEAL.

CONFLICT OF INTERESTS

The authors declare that there are no conflict of interests.

AUTHOR CONTRIBUTIONS

Florian Gothe: conceptualization (equal); data curation (lead); writing—original draft (lead). **Jonathan Gehrig**: investigation (lead); writing—review and editing (equal). **Christina K. Rapp**: data curation (supporting); formal

analysis (supporting); visualization (supporting). **Katrin Knoflach**: data curation (supporting); visualization (supporting). **Simone Reu-Hofer**: investigation (equal); visualization (equal); writing review and editing (supporting). **Florian Laenger**: investigation (supporting); writing—review and editing (supporting). **Dirk Schramm**: data curation (supporting); writing review and editing (supporting). **Julia Ley-Zaporozhan**: investigation (supporting); visualization (supporting); writing review and editing (supporting). **Stephan Ehl**: funding acquisition (equal); supervision (equal); writing review and editing (equal). **Nicolaus Schwerk**: data curation (supporting); visualization (supporting). **Laura Faletti**: methodology (lead); supervision (lead); writing—original draft (supporting); writing—review and editing (equal). **Matthias Griese**: conceptualization (equal); funding 7acquisition (equal); supervision (equal); writing review and editing (equal).

DATA AVAILABILITY STATEMENT

The data that support the findings of this study are available from the corresponding author upon reasonable request.

ORCID

Florian Gothe https://orcid.org/0000-0003-0421-6610
Dirk Schramm https://orcid.org/0000-0002-0440-4737
Matthias Griese https://orcid.org/0000-0003-0113-912X

REFERENCES

1. Flanagan SE, Haapaniemi E, Russell MA, et al. Activating germline mutations in STAT3 cause early-onset multi-organ autoimmune disease. *Nat Genet*. 2014;46(8):812-814. https://doi.org/10.1038/ng.3040
2. Milner JD, Vogel TP, Forbes L, et al. Early-onset lymphoproliferation and autoimmunity caused by germline STAT3 gain-of-function mutations. *Blood*. 2015;125(4):591-599. https://doi.org/10.1182/blood-2014-09-602763
3. Fabre A, Marchal S, Barlogis V, et al. Clinical aspects of STAT3 gain-of-function germline mutations: a systematic review. *J Allergy Clin Immunol Pract*. 2019;7(6):1958-1969. https://doi.org/10.1016/j.jaip.2019.02.018
4. Faletti L, Ehl S, Heeg M. Germline STAT3 gain-of-function mutations in primary immunodeficiency: impact on the cellular and clinical phenotype. *Biomed J*. 2021;S2319-4170(21):00017-2. https://doi.org/10.1016/j.bj.2021.03.003
5. Jägle S, Heeg M, Grün S, et al. Distinct molecular response patterns of activating STAT3 mutations associate with penetrance of lymphoproliferation and autoimmunity. *Clin Immunol*. 2020;210(108316):108316. https://doi.org/10.1016/j.clim.2019.108316
6. Silva-Carmona M, Vogel TP, Marchal S, et al. Successful treatment of interstitial lung disease in STAT3 gain-of-function using JAK inhibitors. *Am J Respir Crit Care Med*. 2020;202:1-15. https://doi.org/10.1164/rccm.201906-1204le
7. Cortes-Santiago N, Forbes L, Vogel TP, et al. Pulmonary histopathology findings in patients with STAT3 gain of function syndrome. *Pediatr Dev Pathol*. 2021;24(3):227-234. https://doi.org/10.1177/1093526620980615
8. Wanin S, Malka-Ruimy C, Deschildre A, et al. Usefulness of bronchoalveolar lavage in a French pediatric cohort with hypersensitivity pneumonitis. *Pediatr Pulmonol*. 2020;55(1):136-140. https://doi.org/10.1002/ppul.24546
9. Pechkovsky DV, Prêle CM, Wong J, et al. STAT3-mediated signaling dysregulates lung fibroblast-myofibroblast activation and differentiation in UIP/IPF. *Am J Pathol*. 2012;180(4):1398-1412. https://doi.org/10.1016/j.ajpath.2011.12.022
10. Waters DW, Blokland KEC, Pathinayake PS, et al. Fibroblast senescence in the pathology of idiopathic pulmonary fibrosis. *Am J Physiol Lung Cell Mol Physiol*. 2018;315(2):L162-L172. https://doi.org/10.1152/ajplung.00037.2018
11. Waters DW, Blokland KEC, Pathinayake PS, et al. STAT3 regulates the onset of oxidant-induced senescence in lung fibroblasts. *Am J Respir Cell Mol Biol*. 2019;61(1):61-73. https://doi.org/10.1165/rcmb.2018-0328OC
12. Zhang Z, Gothe F, Pennamen P, et al. Human interleukin-2 receptor β mutations associated with defects in immunity and peripheral tolerance. *J Exp Med*. 2019;216(6):1311-1327. https://doi.org/10.1084/jem.20182304
13. Bezrodnik L, Caldirola MS, Seminario AG, Moreira I, Gaillard MI. Follicular bronchiolitis as phenotype associated with CD25 deficiency. *Clin Exp Immunol*. 2014;175(2):227-234. https://doi.org/10.1111/cei.12214
14. Gambineri E, Ciullini Mannurita S, Hagin D, et al. Clinical, immunological, and molecular heterogeneity of 173 patients with the phenotype of immune dysregulation, polyendocrinopathy, enteropathy, X-linked (IPEX) syndrome. *Front Immunol*. 2018;9:2-5. https://doi.org/10.3389/fimmu.2018.02411
15. Schwab C, Gabrysch A, Olbrich P, et al. Phenotype, penetrance, and treatment of 133 cytotoxic T-lymphocyte antigen 4–insufficient subjects. *J Allergy Clin Immunol*. 2018;142(6):1932-1946. https://doi.org/10.1016/j.jaci.2018.02.055
16. Shamriz O, Shadur B, Nasereddin A, et al. Respiratory manifestations in LPS-responsive beige-like anchor (LRBA) protein-deficient patients. *Eur J Pediatr*. 2018;177:1163-1172.
17. Liu Y, Jesus AA, Marrero B, et al. Activated STING in a vascular and pulmonary syndrome. *N Engl J Med*. 2014;371(6):507-518. https://doi.org/10.1056/NEJMoa1312625
18. Watkin LB, Jessen B, Wiszniewski W, et al. COPA mutations impair ER-Golgi transport and cause hereditary autoimmune-mediated lung disease and arthritis. *Nature Genet*. 2015;47(6):654-660 http://www.nature.com/doifinder/10.1038/ng.3279%5Cnpapers3://publication/doi/10.1038/ng.3279
19. Lepelley A, Martin-Niclós MJ, Le Bihan M, et al. Mutations in COPA lead to abnormal trafficking of STING to the Golgi and interferon signaling. *J Exp Med*. 2020;217(11), https://doi.org/10.1084/JEM.20200600
20. Magg T, Okano T, Koenig LM, et al. Heterozygous OAS1 gain-of-function variants cause an autoinflammatory immunodeficiency. *Sci Immunol*. 2021;6(60):eabf9564. https://doi.org/10.1126/sciimmunol.abf9564
21. Kim H, De Jesus AA, Brooks SR, et al. Development of a validated interferon score using nanostring technology. *J Interferon Cytokine Res*. 2018;38(4):171-185. https://doi.org/10.1089/jir.2017.0127
22. Gutiérrez M, Scaglia P, Keselman A, et al. Partial growth hormone insensitivity and dysregulatory immune disease associated with de novo germline activating STAT3 mutations. *Mol Cell Endocrinol*. 2018;473:166-177. https://doi.org/10.1016/j.mce.2018.01.016
23. Fabre A, Marchal S, Forbes LR, et al. STAT3 gain of function: a new kid on the block in interstitial lung diseases. *Am J Respir Crit Care Med*. 2018;197(11):e22-e23. https://doi.org/10.1164/rccm.201707-1500IM

SUPPORTING INFORMATION

Additional supporting information may be found in the online version of the article at the publisher's website.

How to cite this article: Gothe F, Gehrig J, Rapp CK, et al. Early-onset, fatal interstitial lung disease in STAT3 gain-of-function patients. *Pediatric Pulmonology*. 2021;56:3934-3941. https://doi.org/10.1002/ppul.25684